Enhanced Self-Assembly of Pyridine-Capped CdSe Nanocrystals on Individual Single-Walled Carbon Nanotubes

Qingwen Li,[†] Baoquan Sun,[‡] Ian A. Kinloch,[†] Dan Zhi,[†] Henning Sirringhaus,[‡] and Alan H. Windle*,[†]

Department of Materials Science and Metallurgy, University of Cambridge, Pembroke Street, Cambridge, CB2 3QZ U.K., and Cavendish Laboratory, University of Cambridge, Madingley Road, Cambridge, CB3 0HE U.K.

We present a simple, noncovalent method for anchoring CdSe quantum dots (QDs) onto individual single-walled carbon nanotubes (SWNTs) through a ligand-exchange approach. Trioctylphosphine oxide (TOPO)-capped CdSe quantum dots were prepared, and the cap was then exchanged for pyridine (Py). It was found that the pyridine-capped quantum dots assembled much more effectively onto the SWNTs compared to the original TOPO-capped quantum dots. The density of the coverage of the quantum dots on the nanotubes was controlled through varying the concentration of the quantum dot solution and the reaction time. Spectroscopic studies indicated that the favorable formation of (Py-QD)−SWNT conjugates resulted from the $\pi-\pi$ stacking interaction between the electron-rich SWNTs and the aromatic pyridine-capped quantum dots. Furthermore, the photoluminescence quenching of the quantum dots due to their interaction with the nanotubes suggests that the electron transfer from the quantum dots to the nanotubes was enhanced by using the pyridine cap.

1. Introduction

Single-walled carbon nanotubes (SWNTs) are potential building blocks for nanoscale devices on account of their unique combination of electronic, mechanical, and structural properties. However, methods still need to be developed for producing the complex nanotube architectures required by these devices.[1,2] The production methods being researched include manipulating the nanotubes' morphology by bending them,[3] or by forming T-[4] and Y-shaped[5] junctions. Alternatively, organic,[6] inorganic,[7] and macromolecular species[8] are attached to the nanotubes, forming heterojunctions. The assembly of semiconducting quantum dots (QDs) onto nanotubes is an attractive method for forming such heterogeneous structures.[9−11] In particular, quantum dots can control the properties because they can be viewed as artificial atoms with tuned electronic states through size confinement.

The advantages of using nanotubes instead of other nanowires for such junctions are that nanotubes can carry higher current densities,[12] display ballistic transport, and have a significant number of delocalized electrons.

The strategies reported so far for producing quantum dot−SWNT structures have involved the chemical functionalization of nanotubes followed by the covalent coupling of ligand-stabilized quantum dots onto the tubes' surfaces.[10,13−16] The main problems with this approach are the low efficiency of the chemical functionalization, the unpredictable effect of such treatment on the electronic properties of the nanotubes, and the nonuniform assembly of the quantum dots. Herein, we report on the noncovalent assembly of CdSe QDs onto SWNTs through a simple ligand-exchange approach. Trioctylphosphine oxide (TOPO)-capped CdSe QDs were prepared, and the TOPO cap was then exchanged for pyridine (Py). It was found that the pyridine-capped quantum dots assembled much more effectively onto SWNTs compared to the original TOPO-capped quantum dots. The effects of the reaction time and the ratio of quantum dots to SWNTs on the assembly process were studied. The resulting coated nanotubes were examined using electron microscopy, atomic force microscopy (AFM), photoluminescence spectroscopy, and Raman spectroscopy. Comparative studies were also made with highly ordered pyrolytic graphite (HOPG) and multiwalled carbon nanotubes (MWNTs) in order to under-

(1) Keren, K.; Krueger, M.; Gilad, R.; Ben-Yoseph, G.; Braun, E. *Science* **2002,** *297,* 72.
(2) Avouris, P. *MRS Bull.* **2004,** 403.
(3) Yao, Z.; Postma, H. W. C.; Dekker, C. *Nature* **1999,** *402,* 273.
(4) Ponomareva, I.; Chernozatonskii, L. A.; Andriotis, A.; Menon, M. *New J. Phys.* **2003,** *5,* 119.
(5) Zhou, D.; Seraphin, S. *Chem. Phys. Lett.* **1995,** *238,* 285.
(6) Shiral Fermando, K.; Lin, Y.; Sun, Y. P. *J. Am. Chem. Soc.* **2004,** *126,* 10234.
(7) Banerjee, S.; Wong, S. S. *Nano Lett.* **2002,** *2,* 195.
(8) Chen, R. J.; Zhang, Y.; Wang, D.; Dai, H. *J. Am. Chem. Soc.* **2001,** *123,* 3838.
(9) Landi, B.; Castro, S.; Ruf, H.; Evans, C.; Raffaelle, R. *Sol. Energy Mater. Sol. Cells* **2004,** ASAP article.
(10) Banerjee, S.; Wong, S. S. *J. Am. Chem. Soc.* **2003,** *125,* 10342.
(11) Ellis, A.; Vijayamohanan, K.; Goswami, R.; Ajayan, P.; Ramanath, G. *Nano Lett.* **2003,** *3,* 279.
(12) Hertel, T.; Martel, R.; Avouris, P. *J. Phys. Chem. B* **1998,** *102,* 910.
(13) Haremza, J. M.; Hahn, M. A.; Krauss, T. D. *Nano Lett.* **2002,** *2,* 1253.
(14) Ravindran, S.; Chaudhary, S.; Colburn, B.; Ozkan, C. S. *Nano Lett.* **2003,** *3,* 447.
(15) Ravindran, S.; Bozhilov, K. N.; Ozkan, C. S. *Carbon* **2004,** *42,* 1537.
(16) Azamian, B. R.; Coleman, K. S.; Hanson, N.; Green, M. H. *Chem. Commun.* **2002,** 366.

stand the interaction between the nanotubes and the quantum dots. It is hoped that this work will lead to the development of optoelectronic devices based on the CdSe quantum dot-coated nanotubes.

2. Experimental Section

The CdSe quantum dots were synthesized by a method adapted from that of Murray et al.,[17] who injected an organometallic precursor into a hot coordinating solvent. The solution of the organometallic was prepared in a glovebox by completely dissolving 0.16 g of Se into 2.4 g of tributylphosphine (TBP). Dimethylcadmium (0.4 g) and a further 6.6 g of TBP were then added to the mixture, and the solution was sealed in a vial with a rubber septum. A flask containing 6 g of technical grade TOPO was heated to 350 °C under an argon atmosphere while the TOPO was being stirred. Once the TOPO reached that temperature, we injected 3 mL of the cooled stock solution into the flask. The resulting solution was held at 300 °C until nanocrystals of the required size were grown. After cooling the solution to 50 °C, we added 10 mL of methanol to precipitate the nanocrystals. The product was then centrifuged, and was washed with methanol five times, which was sufficient for removing any excess ligand. The resulting TOPO-capped CdSe quantum dots were finally dissolved, and were kept in hexane. The TOPO ligand was exchanged for pyridine by refluxing the particles (60 mg) in anhydrous pyridine (15 mL) at 118 °C under argon for 24 h. Optical adsorption spectroscopy and atomic force microscopy found that the average diameters of the pyridine-capped quantum dots ranged from 2.5 to 3.5 nm. The ligand replacement did not have a large influence on the absorption spectrum of the quantum dots.

The SWNTs were synthesized by the catalytic vapor deposition (CVD) of methane over an iron catalyst held on a MgO support, as described in detail elsewhere.[18] The as-produced SWNTs were dispersed into individual entities by first exfoliating the tubes in a NaOH ethanol solution and then dispersing them in 1,1,2,2-tetrachloroethane.[19] This dispersion was spin-coated onto a clean silicon wafer, and was annealed at 300 °C for 30 min in order to remove any residual solvent.

The quantum dots were deposited on various graphitic surfaces in order to understand their interaction with carbon. Initial experiments were conducted by immersing highly ordered pyrolytic graphite (HOPG) into quantum dot solutions, followed by thoroughly washing the graphite with solvent to remove any excess dots. Quantum dots were introduced to SWNTs by either adding nanotubes to the quantum dot solution or immersing nanotube-coated silicon wafers into the quantum dot solutions. Finally, multiwalled carbon nanotubes (MWNTs) from Tsinghua University, with an average outer diameter of ~10 nm and purity of >90%, were reacted with the quantum dots as a comparison to the SWNTs. The quantum dot−carbon interactions were studied with UV−visible and IR spectroscopies, atomic force microscopy (AFM, Digital Instruments Nanoscope IIIa), micro-Raman spectroscopy (Renishaw 1000), and high-resolution transmission electron microscopy (HRTEM).

3. Results and Discussion

3.1. Interaction of the CdSe QDs with a Hydrophobic HOPG Surface. The TOPO ligand is commonly used to

(17) Murray, C. B.; Norris, D. J.; Bawendi, M. G. *J. Am. Chem. Soc.* **1993**, *115*, 8706.
(18) Li, Q.; Yan, H.; Zhang, J.; Liu, Z. *J. Mater. Chem.* **2002**, *12*, 1179.
(19) Li, Q.; Kinloch, I. A.; Windle, A. H. *Chem. Commun.* **2005**, *26*, 3283−3285.
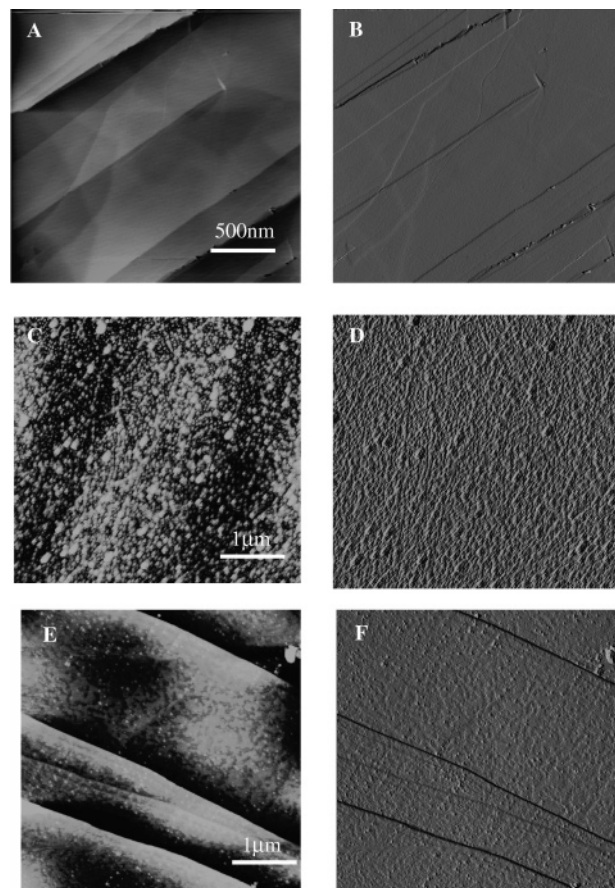

Figure 1. AFM images of the HOPG surfaces before and after interaction with the quantum dots. Height (A) and phase (B) images of the as-cleaned HOPG surface; height (C) and phase (D) images of the HOPG surface after interaction with TOPO-QDs; height (E) and phase (F) images of the HOPG surface after interaction with Py-QDs.

cap and passivate the surface of CdSe quantum dots for a variety of reasons: it coordinates the surface cadmium atoms, forms a protective layer against sintering, provides solubility, and maintains good optical properties. By refluxing the TOPO-capped CdSe QDs in a pyridine solvent, we can replace more than 90% of the TOPO with pyridine.[14] This exchange of ligands modifies the surface states of the quantum dots and increases their conductivity; consequently, this promotes electron transport through their nanocrystals.[15] Also, replacing the TOPO with pyridine changes the outer layer of the quantum dots from a hydrophobic alkyl tail to an aromatic conjugated tail. As a result of this change of ligand, the pyridine-capped quantum dots' behavior on hydrophobic carbon surfaces will be different than that of the TOPO-capped dots.

Highly oriented pyrolytic graphite (HOPG) is a high-purity carbon with a smooth, hydrophobic surface. Therefore, it is an ideal substrate on which to use AFM for studying the interaction of carbon with other species. Panels A and B of Figure 1 show typical AFM images (height and phase contrast) of a freshly cleaved HOPG surface. The atomic steps 0.2−0.3 nm in height observed in these samples are grain boundaries between the graphite crystals. Large aggregates and some small discrete nanoparticles were deposited on the HOPG surface after it was immersed in a hexane solution of TOPO-QDs (0.2 mg/mL) for 2 min (see the Supporting Information Figure 1). The height of the isolated

nanoparticles (3.5 nm) was consistent with the value of the quantum dot's size as determined by UV spectroscopy, suggesting that the particles were individual quantum dots. The large features on the surface were aggregates of the quantum dots, with the average height of the aggregates being nearly twice that of discrete nanoparticles, implying that two layers are stacked. Upon an increase in the adsorption time to 5 min or longer, the HOPG surface became densely covered by the layered aggregates of quantum dots (Figure 1C,D). It is therefore apparent that the quantum dots do not form a uniform coating on the HOPG due to the unspecific TOPO−graphite interaction. Interestingly, it should be noted that although there was no difference in density of the coverage between the basal plane and edges of the HOPG surface, the basal plane did favor the deposition of the large aggregates rather than the isolated dots.

In contrast, after 5−10 min of immersion, the Py-QDs uniformly coated the HOPG such that the surface still appeared smooth. This coating also followed the HOPG's surface topology, with the atomic steps being matched by the coating (Figure 1E,F). Section analysis revealed that the height of the adsorbed aggregates was less than 3 nm, implying a monolayer of Py-QDs on the HOPG's surface. (The Py-capped quantum dots were smaller in diameter than the TOPO-capped ones because of the smaller ligand.[20])

The difference in behavior of the two different ligands can be understood by considering the surface chemistry of the quantum dots: in the TOPO-capped quantum dots, the phosphine oxide group coordinates to the surface of the quantum dot and the alkyl group stretched out. TOPO-QDs are therefore hydrophobic and soluble in hexane. Furthermore, the alkyl tails mean that the TOPO-QDs will interact poorly with a graphite surface. When the TOPO ligand is exchanged for pyridine, the surface of the quantum dots becomes polar, making them insoluble in hexane but soluble in polar solvents such as pyridine, alcohol, and chloroform. Importantly, the exchange for pyridine also makes the quantum dots' surfaces aromatic, which encourages them to form a monoloayer on a graphite surface through $\pi-\pi$ stacking.

3.2. Enhanced Assembly of CdSe QDs onto Individual SWNTs. SWNTs can be considered as a single sheet of graphite rolled up to form a seamless tubular structure. Thus, the surface properties of SWNTs are analogous to that of HOPG, ignoring any high surface-energy effects from the curvature. Ultrasonically dispersing a small amount of SWNTs into a Py-QD 2-propanol solution changed the quantum dot solution's initial orange color to a light gray within a few minutes. It is believed that this color change occurred because of the Py-QDs self-assembling onto the SWNTs and subsequently being quenched, as explained later. Once the orange color was eliminated, only the gray color from the blackness of the SWNTs was left. However, no color change was observed when nanotubes were added to a TOPO-QD toluene solution or a 2-propanol solution in which only some of the TOPO ligands had been exchanged
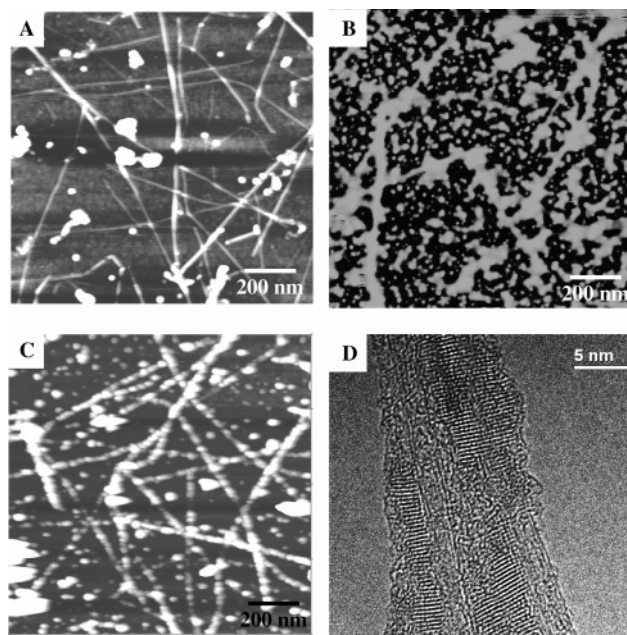
(20) Rosen, M. *Surfactants and Interfacial Phenomena*; John Wiley and Sons: New York, 1989.

Figure 2. AFM images of the individual SWNTs reacted with the TOPO-QDs and the Py-QDs: (A) well-dispersed individual SWNTs on the Si surface; (B) nonspecific adsorption of TOPO-capped quantum dots on SWNTs and silicon; (C) enhanced self-assembly of Py-QDs on individual SWNTs (scale bar is 200 nm); (D) TEM image showing the coating of Py-QDs upon a SWNT bundle.

for pyridine. Therefore, it appears that there is little interaction between TOPO caps and nanotubes, and a $\pi-\pi$ interaction is required for attaching the quantum dots to the tubes.

To further investigate the interaction of the different ligands with the SWNTs, individual SWNTs were spin coated onto a silicon surface, and were introduced to quantum dot solutions. AFM analysis found that the as-spun samples prior to the introduction of quantum dots possessed regions with a significant number of well-dispersed individual nanotubes, with the tubes' diameters ranging from 0.8 to 2.5 nm (Figure 2A). These SWNTs had a good coherent affinity for silicon surface, and remained on the substrate even when being washed or placed under a high-pressure nitrogen gas stream.

The spin-coated wafers became densely covered by quantum dot nanocrystals after being immersed in a TOPO-QD solution (0.01 mg/mL) for 5 min and thoroughly washed in hexane (Figure 2B). The adsorption of the TOPO-QDs occurred over the entire surface and was nonspecific to SWNTs, which is consistent with the results from the HOPG. The quantum dot coating was thicker on the wider nanotubes, and was not uniform, especially on the very thin tubes (0.66 nm diameter).

Figure 2C shows the AFM topography of the SWNTs after interaction with a dilute solution of Py-QDs for 5 min. The Py-QDs had a higher selectivity for the SWNTs than the TOPO-QDs, and preferably assembled on the nanotubes rather than on the silicon. Cross-sectional analysis indicated each tube was covered by a quantum dot monolayer, which was also confirmed by HRTEM (Figure 2D). In addition to the earlier discussion on HOPG, it can be concluded that the pyridine-capped CdSe QDs showed good affinity for

Enhanced Self-Assembly of Pyridine-Capped CdSe Nanocrystals

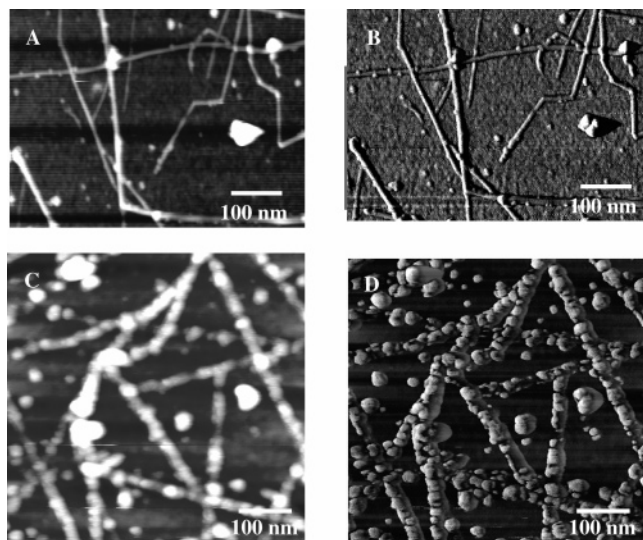*Chem. Mater., Vol. 18, No. 1, 2006* **167**

Figure 3. AFM images showing Py-QDs anchored onto individual SWNTs as discrete particles (A and B) and as a uniform coating (C and D).

graphene structures because of their $\pi-\pi$ stacking interactions.

It was found that the density of the quantum dot coverage on individual SWNTs could be controlled easily by varying the concentration of the Py-QD solution and the immersion time (Figure 3). For a dilute quantum dot solution (<0.01 mg/mL) with an immersion time of less than 5 min, some small particles assembled on the smaller nanotubes (average tube diameter < 1 nm). Comparative results from pure pyridine revealed that these small particles were not impurities from the solvent but rather quantum dots. When the SWNTs were immersed for longer periods, each tube became densely wrapped in quantum dots (Figure 3C,D). In this way, CdSe QDs can either self-assemble as discrete particles or as a uniform coating upon the nanotubes.

3.3. Spectroscopic Studies. Figure 4A shows the UV–vis adsorption spectra obtained from a 2-propanol solution of Py-QDs, the SWNTs dispersed on a quartz substrate, and the SWNT–(Py-QD) conjugates. The Py-QDs and SWNTs have characteristic exciton adsorption peaks at 523 and 269 nm, respectively. After interaction, the adsorption peak from the SWNTs remained as before, but the quantum dots' adsorption peak blue-shifted slightly and broadened. The intensity of the quantum dots' peaks were also reduced compared to that in solution, with the decrease being due to a combination of a lower concentration of quantum dots and the nanotubes absorbing some of the signal. Figure 4B shows the FTIR spectra from the pyridine, Py-QDs, Py-SWNTs, and SWNT–(Py-QD) conjugates. The characteristic peaks of pyridine are located at 1581, 1437, 1030, and 991 cm^{-1}, and are attributed to the symmetric and asymmetric ring breathing and the C–C and C–N stretching modes, respectively. Pyridine is a good electron donor due to the presence of a pair of isolated nitrogen electrons that is delocalized over its entire aromatic ring. CdSe quantum dots show a good electron affinity, meaning that the nitrogen readily coordinates with them to form a stable complex. As a consequence, the three characteristic bands of pyridine were shifted to 1611, 1485, and 1059 cm^{-1} for the Py-QD complex. When the SWNTs were treated with pyridine vapor or were in
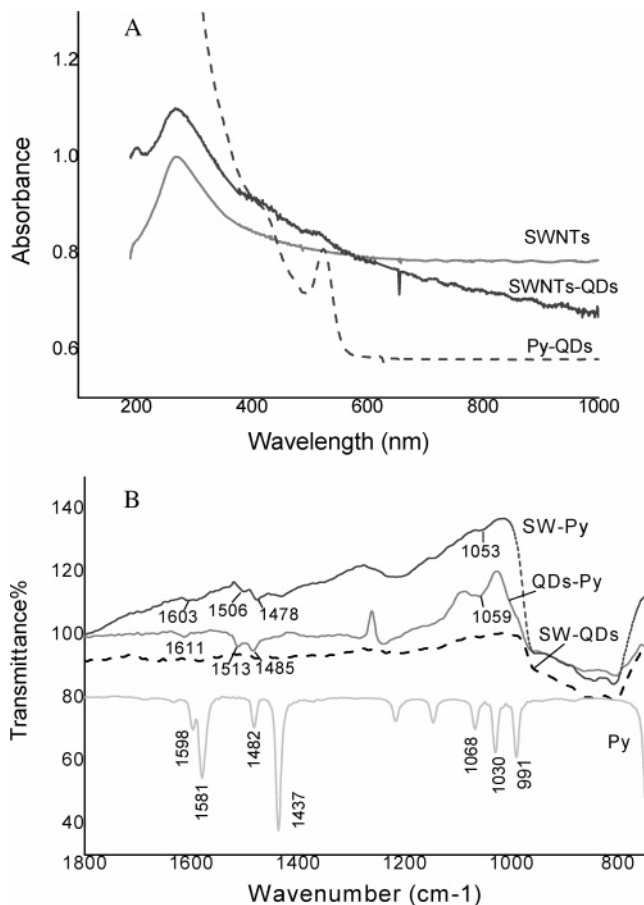

Figure 4. UV–vis adsorption spectra (A) and FTIR spectra (B) of Py-QDs, SWNTs, and SWNT–QD conjugates.

solution, the characteristic bands of pyridine shifted, indicating that pyridine also had a strong interaction with the SWNTs, probably through conjugated $\pi-\pi$ stacking. Therefore, it is concluded that the good interactions of the pyridine with both the QDs and the SWNTs are vital for the self-assembly process observed.

Raman spectroscopy was used to investigate the interaction between the CdSe QDs and SWNTs coated on the silicon wafers. An excitation laser of 514 nm was used, which is close to the characteristic adsorption peak at 523 nm for the Py-QDs. As shown in Figure 5, strong and broad photoluminescence emission of quantum dots was observed at the lower wavenumbers (below 1000 cm^{-1}). This photoluminescence emission drowned any other signals from the quantum dots. However, when a 635 nm laser was used, which is away from the quantum dots' fluorescence wavelength, the two characteristic Raman peaks of CdSe were found at 205 and 410 cm^{-1}, which correspond to the CdSe longitudinal optical (LO) phonon and its overtone (spectrum not shown). The Raman spectrum of the SWNT–QD conjugates was significantly different from those of the individual tubes and dots. In particular, the photoluminescence emission of the Py-QDs was significantly quenched by the nanotubes, and what remained of the band was shifted to higher wavenumbers due to the quantum dot–nanotube interaction.

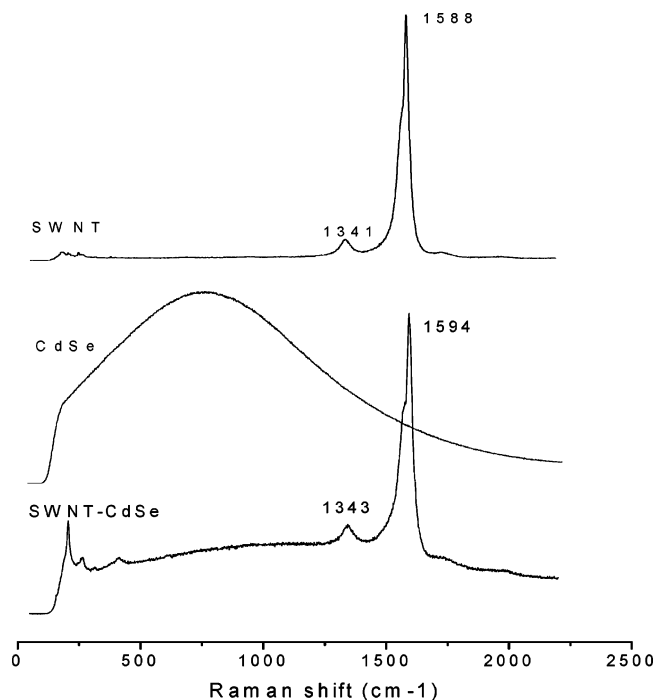The photoluminescence quenching of the quantum dots at the lower wavenumbers also revealed three peaks at 204,

Figure 5. Raman spectra of the Py-QDs, SWNTs, and SWNT−QD conjugates taken using a 514 nm excitation laser. The broad peak in the lower two spectra is the photoluminescence peak from the quantum dots. The quenching and shift of this peak can be observed for the SWNT−QD conjugate. The peaks at ∼1340 and ∼1590 cm^{-1} are the D and G bands, respectively, from the carbon nanotubes.

261, and 409 cm^{-1} in the Raman spectra that were previously hidden by the photoluminescence peak (Figure 5). These three peaks were not the radial breathing mode (RBM) peaks of SWNTs, as their relative intensities (compared to the G peak of the SWNTs) were stronger and their peak positions different. Therefore, the peaks were from the photoluminescence rather than the SWNTs. This assumption was further confirmed by the peak also being present in the Raman spectra of the Py-Qd-coated MWNTs (Figure 2 in the Supporting Information). In addition, because of the attachment of Py-QDs onto the sidewalls of SWNTs, the original G peak at 1588 cm^{-1} and D peak at 1341 cm^{-1} of the uncoated SWNTs were shifted to 1594 and 1343 cm^{-1} respectively. However, the adsorption of pyridine on SWNTs did not result in such a large Raman shift of these two peaks, indicating that the assembly of the rigid and heavy QD nanocrystals onto the tubes deformed the sidewall of SWNTs.

Scheme 1 shows the energies in the nanotube−quantum dot system. The valence band (E_v) and conduction band (E_c) energy levels for the as-prepared CdSe quantum dots are taken to be 5.5 eV and 3.13 eV, respectively.[21] The energy bands for the semiconducting SWNTs (s-SWNTs) are taken to be E_v = 5.4 eV and E_c = 4.8 eV.[22,23] The Fermi level (E_f) of metallic SWNTs (m-SWNTs) is taken to be 4.5−5.0 eV.[22,23] The photoluminescence of the quantum dots is due to the irradiative decay path from their excited state to their ground state. Given that the nanotubes quenched the CdSe

(21) Kucur, E.; Riegler, J.; Urban, G.; Nann, T. *J. Chem. Phys.* **2003**, *119*, 2333.
(22) Kazaoui, S.; Minami, N.; Matsuda, N.; Kataura, H.; Achiba, Y. *Appl. Phys. Lett.* **2001**, *78*, 3433.
(23) Shiraishi, M.; Ata, M. *Carbon* **2001**, *39*, 1913.

Scheme 1. Energy Level Diagram and Possible Charge-Transfer Process for the Conjugate Complex between CdSe Quantum Dots and Semiconductor SWNT (s-SWNT) or Metal SWNT (m-SWNT)[a]
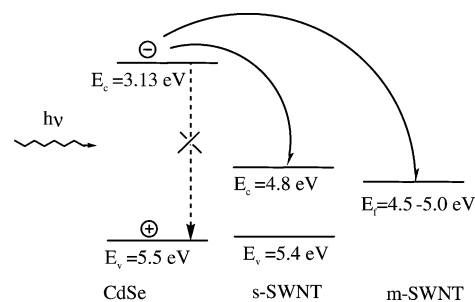
[a] E_v, E_c, and E_f denote valence band, conduction band, and Fermi energy levels, respectively.

quantum dots, the tubes' interaction with the quantum dots must provide an alternative, nonirradiative decay path. It is believed this nonirradiative decay path occurs because the electron affinity between the CdSe quantum dots and the SWNTs is sufficiently different that it allows electron transfer from the quantum dots to the SWNTs.[9] In other words, the formation of SWNT−QD conjugates favors the electron transfer from the quantum dots (donor) to the SWNTs (acceptor) such that the excited electrons entered the SWNTs rather than be emitted as the photoluminescence peak. The smaller size of the pyridine cap compared to that of the TOPO cap and its conjugated structure may account for this enhancement of the electron transfer.

4. Conclusions

We presented a simple and noncovalent method for anchoring CdSe quantum dots onto individual SWNTs. The exchange of the quantum dots' TOPO ligand to pyridine resulted in an increased affinity with hydrophobic carbon surfaces, probably through π−π stacking. Consequently, the quantum dots self-assembled onto individual SWNTs, with no need for any chemical functionalization of the tubes. The quantum dots could form either discrete crystals or a uniform layer on the SWNTs, depending on the ratio of quantum dots to SWNTs and on the reaction time. Raman spectroscopic monitoring of the photoluminescence peak was used to investigate the interaction between the SWNTs and quantum dots. The quenching of this peak in the nanotube−quantum dot assemblies suggests that electron transfer may be favored from the CdSe donor to the SWNT acceptor.

Supporting Information Available: AFM images of the TOPO-capped CdSe on HOPG and Raman spectroscopy of the samples (pdf). This material is available free of charge via the Internet at http://pubs.acs.org.